Angular Dependence of Electron Impact Excitation Cross Sections of O_2

S. TRAJMAR,*† W. WILLIAMS,* AND A. KUPPERMANN†

Division of Chemistry and Chemical Engineering, California Institute of Technology, Pasadena, California 91109

(Received 19 April 1971)

The electron-impact excitation spectrum of O_2 has been studied at 20 and 45 eV impact energies and at scattering angles ranging from 10° to 90°. The angular behavior of the differential scattering cross sections for excitation of the $a\,^1\Delta_g$, $b\,^1\Sigma_g^+$, $B\,^3\Sigma_u^-$ states, for the 9.97 eV ("longest" band), and the 10.29 eV ("second" band) transitions, for the broad feature at 6.1 eV energy-loss (previously assigned to the excitation of the $A\,^3\Sigma_u^+$ state), and for elastic scattering has been determined. The experimentally measured relative differential and integral cross sections for these processes have been approximately normalized to the absolute scale. The intensities of the different transitions in optical and electron-impact spectra are compared and the importance of spin–orbit coupling and exchange processes are discussed. It is found that the energy-loss feature at 6.1 eV in the electron-impact spectrum is mostly due to the excitation of the $c\,^1\Sigma_u^-$ state. This new assignment is supported by the angular and energy dependence of the scattering cross section (and by the intensity pattern found in various electron impact processes).

I. INTRODUCTION

The electron impact excitation of O_2 is of considerable interest in atmospheric chemistry and physics. It is also of particular interest from the point of view of electron scattering in general because the ground electronic state of the molecule is a triplet spin state.

Transitions between the ground ($X\,^3\Sigma_g^-$) and the five lowest known excited ($a\,^1\Delta_g$, $b\,^1\Sigma_g^+$, $A\,^3\Sigma_u^+$, $C\,^3\Delta_u$, and $c\,^1\Sigma_u^-$) states are forbidden[1] by electric and magnetic dipole optical selection rules and also, excepting the $C\,^3\Delta_u$ state, by electric quadruple optical selection rules. These transitions have been observed optically[2] and they occur as the result of spin–orbit interactions. The $X\,^3\Sigma_g^- \rightarrow B\,^3\Sigma_u^-$ transition is optically allowed and is very intense. There are two strong bands at 9.97 ("longest" band) and 10.29 eV ("second" band) which appear in optical spectra,[3,4] but they have not been analyzed and assigned yet. The potential energy curves of the pertinent states of O_2 are shown in Fig. 1.[5]

Geiger and Schröder[6] using 25 KeV electrons observed the $B\,^3\Sigma_u^-$, 9.97, and 10.29 eV excitations (as well as many higher energy transitions) at zero degree scattering angle. At energies of 50, 70, and 512 eV and at low scattering angles (below 15°) Lassettre, *et al.*,[7] observed the excitation of the $B\,^3\Sigma_u^-$ state, the 9.97 and the 10.29 eV bands (as well as many features corresponding to higher excitation energies). At 45 eV and low scattering angles, Skerbele, *et al.*,[8] also detected pure vibrational excitation and the $X\,^3\Sigma_g^- \rightarrow a\,^1\Delta_g$ transition. Schulz and Dowell[9] studied the low impact-energy threshold region by the trapped electron method. They observed pure vibrational excitation to the $v''=1$ through $v''=8$ levels and found excitation of the $a\,^1\Delta_g$ and $b\,^1\Sigma_g^+$ states superimposed on the vibrational features. A peak at 6.1 eV identified as the $X\,^3\Sigma_g^- \rightarrow A\,^3\Sigma_u^+$ transition as well as the Schuman–Runge, the "longest" and "second" bands, also appear in their spectrum. Very recently Konishi, *et al.*,[10] reported integral cross sections for the electron-impact excitation of the $a\,^1\Delta_g$ and $b\,^1\Sigma_g^+$ states of O_2 as well as the sum of the $^3\Sigma^+{}_u$ A and $C\,^3\Delta_u$ integral cross sections for the 20–70 eV impact energy range.

Our investigation was carried out over a wide angular range (20°–90°) and at impact energies (20 and 45 eV) intermediate between that of Schulz and Dowell[9] (threshold) and of Lassettre, *et al.*[7] (50–512 eV). These energy and angular ranges are particularly suited for studying optically forbidden transitions.

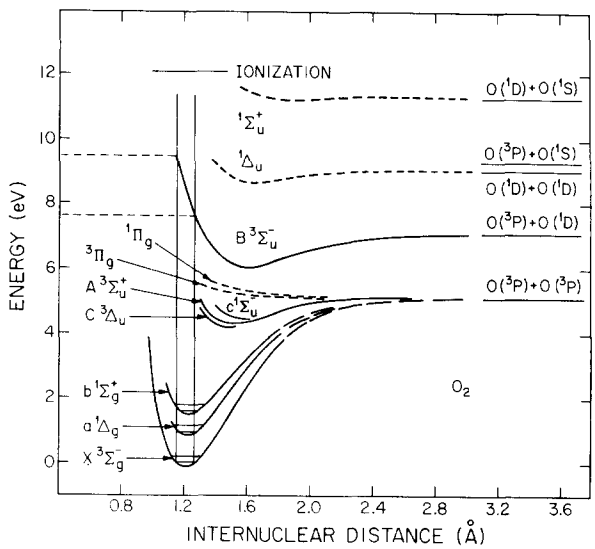

FIG. 1. Potential energy curves for O_2.

Relative differential cross sections (DCS's) and integral cross sections (Q) for elastic scattering and for excitation of the $a\,^1\Delta_g$, $b\,^1\Sigma_g^+$, $c\,^1\Sigma_u^-$, $B\,^3\Sigma_u^-$, 9.97, and 10.29 eV states have been determined at impact energies of 20 and 45 eV, and an approximate calibration to place these cross sections on the absolute scale has been carried out.

II. EXPERIMENTAL

The apparatus and the experimental details have been described earlier.[11] An energy-selected electron

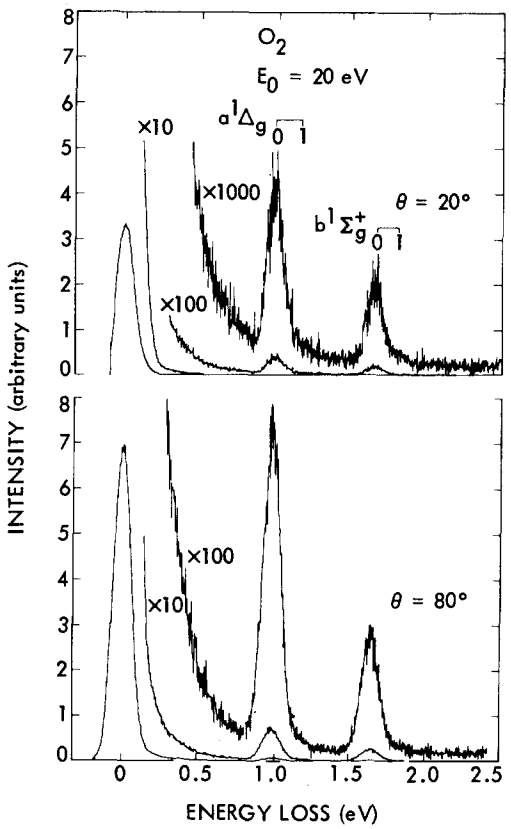

FIG. 2. Energy-loss spectrum of O_2 at 20° and 80° scattering angles. Resolution: 0.10 eV. Impact energy: $E_0 = 20$ eV. Energy loss region 0–2.5 eV.

beam is scattered off a gaseous O_2 target at a pressure of the order of one mtorr. The scattered signal intensity as a function of energy loss is measured at a fixed impact energy (E_0) and scattering angle (θ). The scattering angle can be changed from $-30°$ to 90°. The true zero angle is determined by locating the precise center of symmetry of the scattering intensity for an inelastic feature in the neighborhood of the nominal zero. The impact energy scale was calibrated by determining the location of the 19.31 eV He resonance on our energy scale. This was done by mixing He with the O_2 sample. It was found that the contact potential changed somewhat with the He to O_2 ratio, but it never exceeded 0.050 eV as we went from pure He to a mixture having a 2:1 ratio of O_2 to He. On the basis of this observation, we believe that our impact energies are correct to within ±0.050 eV.

Typical spectra are shown in Figs. 2 and 3. The ratio of the intensities of the inelastic features to that of the elastic one is determined from each spectrum. For the elastic scattering and for the $a\,^1\Delta_g$, $b\,^1\Sigma_g^+$, 9.97, and 10.29 eV excitations, the peak heights were used to get the appropriate intensity ratios. This is an acceptable procedure since at the resolution used (the full width at half maximum for the elastic peak was 0.10 eV) the shapes of these peaks are determined by the instrumental resolution and are all equal and independent of scattering angle. In the case of the 6.1 eV and $B\,^3\Sigma_u^-$ transitions, a correction factor of 19 was introduced to account approximately for the large width of these features compared to the instrumental resolution. This factor was obtained from the ratio of the FWHM of these broad features to that of the narrow peaks. The elastic DCS's were determined by measuring the elastic scattering intensity as a function of scattering angle under identical experimental conditions and by introducing the proper corrections for the change of scattering geometry with scattering angle.[11] From the intensity ratios and from the elastic DCS's, the DCS's for the inelastic processes were obtained in the same arbitrary units as the elastic one. An approximate normalization of the cross sections was carried out by utilizing the total electron–O_2 scattering cross sections measured by Salop and Nakano[12] (at 20 eV) and Sunshine *et al.*[13] (at 45 eV). The DCS's for elastic scattering, excitation of the $a\,^1\Delta_g$, $b\,^1\Sigma_g^+$, $B\,^3\Sigma_u^-$, 6.1, 9.97, and 10.29 eV states were extrapolated to 0° and to 180° and integrated. Contributions from other open channels were estimated from energy loss spectra. The sum of all these integral cross sections was then normalized to the difference of the total electron–O_2 cross section, and the total ionization cross section determined by Rapp and Englander-Golden.[14] The ratios of any two approximate absolute cross sections given in Fig. 6 (or Fig. 7) are more accurate than each

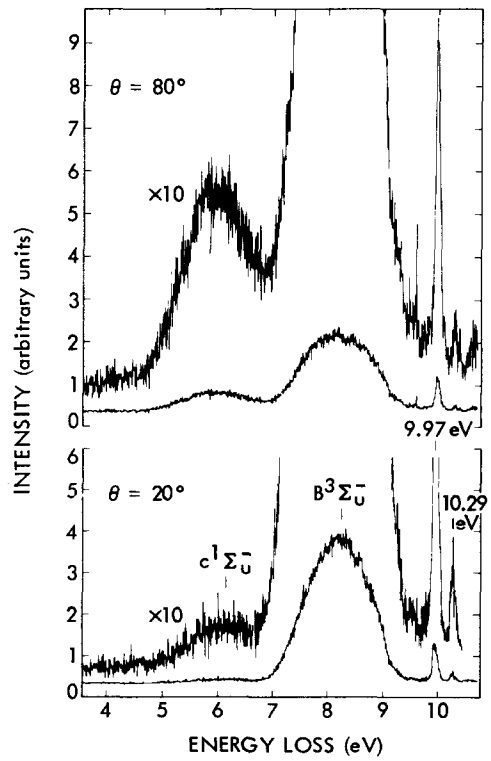

FIG. 3. Same as Fig. 2. Energy loss region 3.5–11 eV.

of the cross sections since the approximate normalization factor cancels out. A similar normalization was used to obtain the results presented in Table I. A more elaborate procedure involving the unfolding of the overlapping features, the calculation of the Franck–Condon factors for the discrete and continuous transitions and a calibration of all cross sections to the absolute scale is in progress and are reported elsewhere.[15]

III. RESULTS AND DISCUSSION

A. Electronic Structure and Optical Spectroscopy of the Lower Excited States

The lowest electronic states of oxygen have the molecular orbital electronic configuration

$$KK(\sigma_g 2s)^2(\sigma_u 2s)^2(\sigma_g 2p)^2(\pi_u 2p)^4(\pi_g 2p)^2.$$

This gives rise to the three states $X\,^3\Sigma_g^-$, $a\,^1\Delta_g$, and $b\,^1\Sigma_g^+$. The first one is the ground electronic state. Starting from it, excitation of the $a\,^1\Delta_g$ state is optically forbidden, violating three electric dipole selection rules: it is spin forbidden, angular momentum forbidden (since $\Delta\Lambda=2$), and parity forbidden (since the initial and final states are both even). Nevertheless, this transition is observed optically constituting the atmospheric infrared bands.[16] The vertical transition energy is of the order of 0.98 eV. The corresponding oscillator strength (f) is relatively weak and is equal to 2.4×10^{-12}. (See Table II for the summary of optical and electron impact transition properties, and appropriate references.) The transition occurs because of spin–orbit coupling and is due to magnetic dipole interaction.[1] The transition from the ground to the $b\,^1\Sigma_g^+$ state also violates three electric dipole selection rules: it is spin forbidden, parity forbidden, and reflection symmetry forbidden (since it connects a Σ^- to a Σ^+ state). This transition is, nevertheless, observed optically and constitutes the atmospheric red bands.[17] It occurs, like the infrared bands, due to spin–orbit coupling and magnetic dipole interaction. Nevertheless, it is stronger than the previous transition by a factor of approximately 20 according to the original estimation of Herzberg and Herzberg.[16] On the basis of the spontaneous emission probabilities this factor is about 500, as can be seen from the data in Table II. The vertical transition energy is 1.63 eV and the corresponding oscillator strength is 2.9×10^{-10}.

The first excited electron configuration is obtained by promoting an electron from the bonding $\pi_u 2p$ orbital to the antibonding $\pi_g 2p$ orbital. This configuration gives rise to the states $A\,^3\Sigma_u^+$, $C\,^3\Delta_u$, $B\,^3\Sigma_u^-$, $^1\Sigma_u^+$, $c\,^1\Sigma_u^-$, and $^1\Delta_u$. Transitions from the ground state to the four states preceded by a Latin character have been observed. Of these four transitions the only one optically allowed is that to the $B\,^3\Sigma_u^-$ state and constitutes the strong Schuman–Runge continuum for which the vertical transition energy is about 8.6 eV [18] and whose oscillator strength is about 0.2. The other three transitions are forbidden. The $X\,^3\Sigma_g^-\rightarrow A\,^3\Sigma_u^+$ transition violates the reflection symmetry selection rule ($\Sigma^-\not\leftrightarrow\Sigma^+$). It has been observed by Herzberg[19] as a set of eleven bands corresponding to $v''=0\rightarrow v'=1$ through 11 excitations[20] (called Herzberg I bands). He found the intensity of these bands weak compared to the $[X\,^3\Sigma_g^-(v''=0)\rightarrow b\,^1\Sigma_g^+(v'=0)]$ transition. To a great extent, this can be attributed to the large difference between the corresponding Franck–Condon factors. The potential energy curve for the $b\,^1\Sigma_g^+$ state is very similar to that of the ground state and 93% of the electronic transition intensity is in the $v''=0$ band. For the $X\,^3\Sigma_g^-\rightarrow A\,^3\Sigma_u^+$ transition the Franck–Condon region is in the continuum and the value of the overlap integral for the discrete bands is very low. Degen and Nicholls[21] measured the relative intensities of 36 bands of the Herzberg I system and determined the relative strengths. Hasson, Nicholls, and Degen[22] carried out absolute measurements for the $v''=0$ progression and placed the strengths of these bands on an absolute scale. According to their results the absolute f-values for the Herzberg I (0–0) and (0–5) bands, e.g., are 2.7×10^{-14} and 5×10^{-11}, respectively. These are smaller by a factor of 10^4 and 6, respectively, than the f-value for the total atmospheric red system. This is consistent with Herzberg's qualitative observations.[19] The integral f-value for the Herzberg I system was estimated by Jarmain and Nicholls as 2×10^{-7}.[23]

The $[X\,^3\Sigma_g^-\ (v''=0)\rightarrow c\,^1\Sigma_u^-\ (v'=1,\ 2\cdots6)]$ and $[X\,^3\Sigma_g^-\ (v''=0)\rightarrow C\,^3\Delta_u\ (v'=5,\ 6)]$ bands were also observed by Herzberg[24] (Herzberg II and Herzberg III bands, respectively). The potential energy curves for the $A\,^3\Sigma_u^+$, $c\,^1\Sigma_u^-$, and $C\,^3\Delta_u$ states have been deter-

TABLE I. Cross sections for e^-+O_2 collisions in Å^2.

Final state	Impact energy: 20 eV, Present work	20 eV, Konishi *et al.*[a]	45 eV, Present work	45 eV, Konishi *et al.*[a]
Elastic	8.0		5.83	
$a\,^1\Delta_g$	0.042	0.02	0.013	0.038
$b\,^1\Sigma_g^+$	0.017	0.0072	0.004	0.017
6.1 eV	0.094	0.043	0.038	0.10
$B\,^3\Sigma_u^-$	0.86		1.15	
9.97 eV	0.013		0.048	
10.29 eV	0.0023		0.017	
Vibrational excitation of ground electronic state[b]	0.040		0.013	
Other electronic states[b]	0.016		0.48	

[a] Reference 10.
[b] Estimated, see text.

TABLE II. Optical and electron impact transition probabilities.

Excited state	Vertical transition energy (eV)	Optical f value	A_{nm} (sec^{-1})	Q [a] (10^{-16} cm^2) E_0-30 eV
$a\,^1\Delta_u$	0.98	2.4×10^{-12} [b]	1.9×10^{-4} [c]	0.02
$b\,^1\Sigma_g^+$	1.63	2.9×10^{-10} [b]	0.1 [d]	0.01
$A\,^3\Sigma_u^+$	6.1	2×10^{-7} [e]	3.2×10^{2} [f]	$\ll0.06$
$c\,^1\Sigma_u^-$	6.1	$<3\times10^{-13}$ [g]	$<1.5\times10^{-3}$ [f]	0.06
$C\,^3\Delta_u$	6.1	$<3\times10^{-14}$ [g]	$<2.4\times10^{-5}$ [f]	$\ll0.06$
$B\,^3\Sigma_u^-$	8.3	0.2 [h]	5.8×10^{8} [f]	1.0

[a] Electron impact excitation cross sections. Present work.
[b] Calculated from A_{nm} using standard formula [Ref. 22, and A. Schadee, J. Quant. Spectry. Radiative Transfer, **7**, 169 (1967)].
[c] A. Vallace Jones and A. W. Harrison, J. Atmospheric Terrest. Phys. **13**, 45 (1958).
[d] Reference 1, p. 24.
[e] Reference 23.
[f] Calculated from f-values using the same formula as in b.
[g] Reference 24. See text for explanation.
[h] Reference 18.

mined by Herzberg and extended to somewhat smaller internuclear distances by Gilmore.[5] All three curves are nearly identical in the internuclear distance range of 1.3 Å upward with a splitting no greater than about 0.2 eV. The equilibrium internuclear distance for all three states is of the order of 1.5–1.6 Å and the dissociation energy of the order of 0.7 eV. The equilibrium internuclear distance of the ground electronic state is 1.2 Å and the vertical Franck–Condon region from its ground vibrational state does not intersect the known portions of the three potential energy curves just discussed. Herzberg found that the Herzberg II system was more than three orders of magnitude weaker than the atmospheric red system and that the Herzberg III system was even weaker than the Herzberg II system. No f values are known for these bands, for the associated continua, or for the overall systems. On the basis of the observations of Herzberg we take $f(c\,^1\Sigma_u^-)\leq 10^{-3}f(b\,^1\Sigma_g^+)$ and $f(C\,^3\Delta_u)\sim10^{-1}f(c\,^1\Sigma_u^-)$.

The transitions from the ground to the $^1\Sigma_u^+$ and $^1\Delta_u$ states probably lie at an energy above 8 eV [19b] where oxygen has several absorption continua and bands and have not yet been identified.

The transitions at 9.97 ("longest" band) and 10.29 eV ("second" band) have been observed by Price and Collins[3] and by Tanaka[4] but no analysis of these bands have been carried out as yet.

B. Electron Impact Excitation

1. The 8.3, 9.97, and 10.29 eV Transitions

For excitation energies between 7 and 10.5 eV the low-energy electron-impact spectrum of oxygen shows three pronounced features. One is a broad intense absorption continuum extending from about 7 to about 9 eV with a maximum at about 8.3 eV as can be seen in Fig. 3. The other two are sharp peaks at 9.97 and 10.29 eV.

The relative differential cross sections of these and other transitions with respect to the 8.3 eV transition as well as the absolute differential cross sections at impact energies of 20 and 45 eV are depicted in Figs. 4–7. From Figs. 6 and 7 it can be seen that the 8.3 eV transition has an angular distribution and a magnitude which is characteristic of optically allowed transitions. The dominant part of it corresponds probably to the Schuman–Runge optical continuum extending over the same range of excitation energies and showing a max-

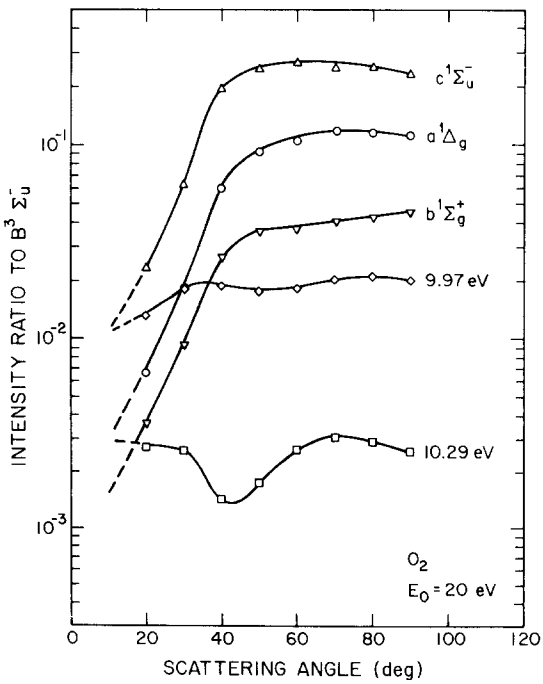

FIG. 4. Intensities of several electronic transitions in O_2 relative to that of the $X\,^3\Sigma_g^-\rightarrow B\,^3\Sigma_u^-$ transition, as a function of scattering angle. The dashed portions of the curves are extrapolations. Resolution: 0.10 eV. Impact energy: $E_0=20$ eV.

imum intensity at about the same position. It is, therefore, identified as being mainly due to the $X\,^3\Sigma_g^- \rightarrow B\,^3\Sigma_u^-$ transition, in agreement with Lassettre, *et al.*[7]

Figures 4–7 indicate that the 9.97 and 10.29 eV transitions have angular distributions very similar to the $X\,^3\Sigma_g^- \rightarrow B\,^3\Sigma_u^-$ transition. They have been observed in electron impact spectra by Lassettre, *et al.*[7] The ratio of the intensity of these bands to that of the $X\,^3\Sigma_g^- \rightarrow B\,^3\Sigma_u^-$ transition does not vary by more than a factor of 3 over the angular range of 20°–90° for both 20 and 45 eV impact energies. From this and their intensities in optical spectra, we conclude that

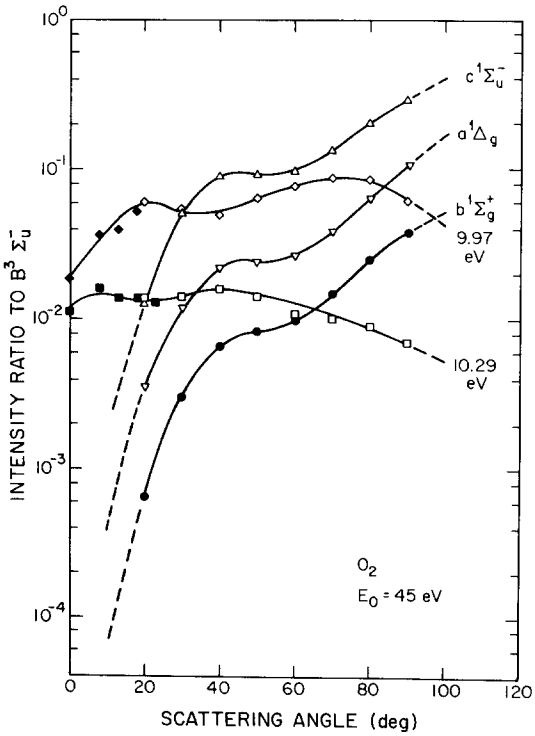

FIG. 5. Same as Fig. 4, except $E_0 = 45$ eV.

they are mostly due to optically allowed transitions ($X\,^3\Sigma_g^- \rightarrow {}^3\Sigma_u^-$ or $X\,^3\Sigma_g^- \rightarrow {}^3\Pi_u$).

2. *The $a\,^1\Delta_g$ and $b\,^1\Sigma_g^+$ Transitions*

As seen in Fig. 2, there are two sharp transitions peaking at 0.98 and 1.63 eV, respectively. They correspond to the infrared ($X\,^3\Sigma_g^- - a\,^1\Delta_g$) and red ($X\,^3\Sigma_g^- - b\,^1\Sigma_g^+$) atmospheric oxygen bands. The corresponding angular distributions depicted in Figs. 4–7 are consistent with the fact they they result from exchange scattering. Skerbele, *et al.*,[8] reported the intensity of the $X\,^3\Sigma_g^- \rightarrow a\,^1\Delta_g$ transition relative to the elastic scattering at an impact energy of 45 eV in the angular range between 3°–12°. They find that in this angular range this intensity ratio is constant and equal

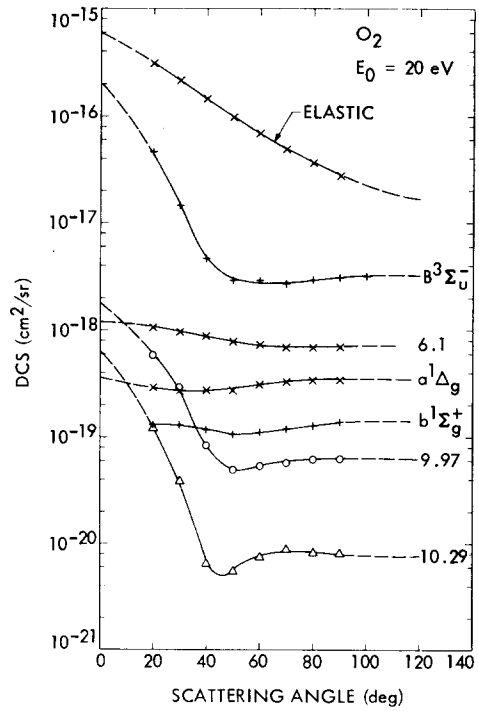

FIG. 6. Differential cross sections (DCS) as a function of scattering angle. Impact Energy: $E_0 = 20$ eV. The solid portions of the curves are drawn through the experimental points; the dashed ones are extrapolations. The absolute ordinance scale includes the approximate normalization described at the end of Sect. II.

to $(1.3 \pm 0.2) \times 10^{-4}$. For the same impact energy we find this same ratio to vary from 2.0×10^{-4} at 10° to 1.3×10^{-2} at 90°, an increase by a factor of 65. This points out the importance of making measurements over a wide angular range in order to establish the

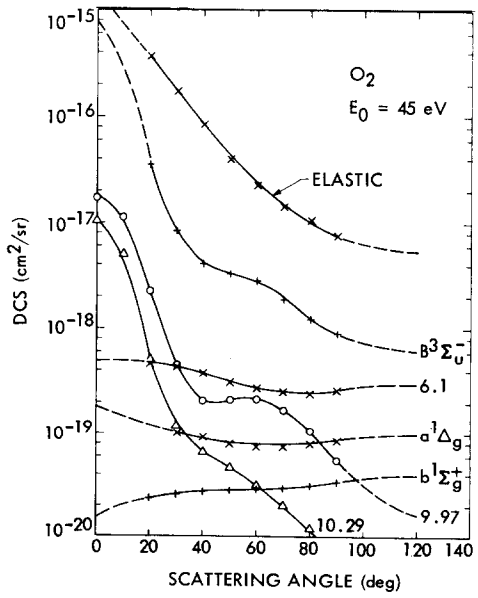

FIG. 7. Same as Fig. 6, except $E_0 = 45$ eV.

characteristic angular dependence of spin forbidden transitions. Our extrapolated $a\,^1\Delta_g$ to elastic scattering intensity ratio at 3° is 1.5×10^{-4} in reasonable agreement with the value found by Skerbele, *et al.*[8]

As pointed out above, transitions from the ground to the $a\,^1\Delta_g$ and $b\,^1\Sigma_g^+$ states occur optically because of spin–orbit coupling. However, the angular distributions we observed indicate that their excitation by low energy electron impact is dominated by an exchange mechanism and, therefore, the contribution of spin–orbit coupling is at best small. Further argument supporting this conclusion is based on the relative intensity of the two transitions. Whereas optically the $X\,^3\Sigma_g^-\rightarrow a\,^1\Delta_g$ transition is about 20 times weaker than the $X\,^3\Sigma_g^-\rightarrow b\,^1\Sigma_g^+$ one,[16] in the electron impact spectra reported here it is about 2 to 10 times stronger, depending on impact energy and scattering angle. This large difference in relative intensities between the two kinds of spectra tend to indicate that a different mechanism is dominant in each case. In addition, the probability for spontaneous emission (A_{nm}) for the $X\,^3\Sigma_g^-\leftarrow b\,^1\Sigma_g^+$ system is about 0.1 sec^{-1} (Ref. 1, p. 25). This may be compared to 10^7–10^8 sec^{-1} for ordinary electric dipole radiations, 10^2–10^3 sec^{-1} for magnetic dipole; and 1 sec^{-1} for electric quadrupole transitions (Ref. 2c, p. 20). The fact that this transition is about eight to nine orders of magnitude weaker than ordinary electric dipole transitions has been attributed to the fact that it occurs as the result of spin–orbit coupling. As can be seen from Fig. 4, in the electron impact spectrum the ratio of the intensity of the $X\,^3\Sigma_g^-\rightarrow b\,^1\Sigma_g^+$ transition to that of the electric dipole optically allowed $X\,^3\Sigma_g^-\rightarrow B\,^3\Sigma_u^-$ transition, at an impact energy of 20 eV, varies from about 3.5×10^{-3} at 20° scattering angle to 4×10^{-2} at a 90° scattering angle. At an impact energy of 45 eV, the corresponding numbers are 6×10^{-4} and 4×10^{-2}. As can be seen from Table I, the integral cross sections for the transition to the $b\,^1\Sigma_g^+$ and $a\,^1\Delta_g$ state at these impact energies are only about two orders of magnitude smaller than for the transition to the $B\,^3\Sigma_u^-$ state. We attribute this enhancement of about six orders of magnitude of the relative probabilities of these two transitions in going from optical to electron impact spectra to a dominance of the exchange mechanism in the latter case.

Konishi *et al.*[10] found that the integral cross sections for the $a\,^1\Delta_g$ and $b\,^1\Sigma_g^+$ excitations, determined from measurements at three angles only (45°, 90°, and 135°), increase slightly in going from 20 to 45 eV impact energy, whereas ours decrease in the same energy range, as seen in Table I. This increase was comparable to their experimental uncertainties. They normalized their elastic cross sections to the total electron–O_2 cross sections of Sunshine, *et al.*,[13] neglecting all inelastic contributions. We attribute the difference between their and our results mainly to the small number of angles used in their measurements and partly to this neglect.

3. *The 6.1 Transition*

As can be seen in Figs. 2 and 3, an absorption continuum is observed starting at about 4.8 eV, reaching the maximum at about 6.1 eV, and decreasing in intensity to about 7 eV at which energy the excitation to the $B\,^3\Sigma_u^-$ state starts dominating. The optically observed Herzberg I bands extend from about 4.4–5.2 eV. It is difficult to study the Herzberg I[19] continuum optically because it is partially overlapped by the strong Schuman–Runge system.[25,26] Ogawa[27] recently measured the continuum optical absorption in this region between the well separated rotational lines of the Schuman–Runge bands. An absorption in this region has been observed by Schulz using the electron trap method.[9a] He correlated its onset with that of the $X\,^3\Sigma_g^-\rightarrow A\,^3\Sigma_u^+$ transition. Hake and Phelps[28] measured the cross section of an energy-loss process in electron swarm experiments and also attributed it to this transition. Finally, Konishi *et al.*[10] assigned the excitation in this region to an overlapping of the transitions to the $A\,^3\Sigma_u^+$ and $C\,^3\Delta_u$ states. These assignments have not been justified by the authors. They are presumably based on the observation that in optical spectra the discrete bands of the $A\,^3\Sigma_u^+$ excitation, although weak compared to the $b\,^1\Sigma_g^+$ system, are much stronger than the bands of the $C\,^3\Delta_u$ or the $c\,^1\Sigma_u$ system. The value of the optical absorption cross section for the Herzberg I system was found to be about 9.7×10^{-24} cm^2 which is approximately six orders of magnitude smaller than that of the Schuman–Runge continuum at around 8.6 eV.[18] On the basis of the observed intensities of the discrete bands of the $A\,^3\Sigma_u^+$, $c\,^1\Sigma_u^-$, and $C\,^3\Delta_u$ excitations, one expects that the contribution to the 6.1 eV continuum from the latter two states is small in optical spectra. In electron impact spectra the peak corresponding to the 6.1 eV continuum is smaller than the peak of the $B\,^3\Sigma_u^-$ continuum only by a factor of 15 (at the 20 to 45 eV impact energies). This enormous gain in the intensity of the 6.1 eV continuum in the electron impact spectrum can be associated with an enhancement due to the spin exchange mechanism. Therefore, we attribute the major contribution to the 6.1 eV broad feature as coming from the $X\,^3\Sigma_g^-\rightarrow c\,^1\Sigma_u^-$ transition.

Figures 4–7 show that the angular dependence of the 6.1 eV transition intensity is very similar in shape to that of the $a\,^1\Delta_g$ and $b\,^1\Sigma_g^+$ transitions. The integral cross sections given in Table I show, furthermore, that at 20 eV impact energy the 6.1 eV transition is 2.2 times more intense than the $X\,^3\Sigma_g^-\rightarrow a\,^1\Delta_g$ transition and about 5.5 times more intense than the $X\,^3\Sigma_g^-\rightarrow b\,^1\Sigma_g^+$ one. At 45 eV impact energy these factors are 2.9 and 9.5, respectively. These observations strongly imply that the 6.1 eV transition is dominated by a spin exchange process. Such a transition would be optically forbidden only by the spin multiplicity selection rule

and would therefore be expected to be more intense, by electron impact, than the transitions to the $a\,^1\Delta_g$ and $b\,^1\Sigma_g^+$ states, as indeed observed. The potential energy curves for the $A\,^3\Sigma_u^+$, $C\,^3\Delta_u$, and $c\,^1\Sigma_u^-$ states are known only at internuclear distances larger than those corresponding to a vertical transition from the classical region of the ground vibrational state and they are nearly identical. Therefore, even for the vertical Franck–Condon band it is not expected that one will be able to distinguish these transitions on the basis of the predicted position and shape of the corresponding energy-loss continua. The main criteria would therefore have to be the corresponding angular distributions and, as indicated above, this strongly points to the $X\,^3\Sigma_g^- \rightarrow c\,^1\Sigma_u^-$ assignment. Two additional states, $^3\Pi_g$ and $^1\Pi_g$, are predicted to exist slightly above this 6.1 eV group, corresponding to the promotion of a $\sigma_g 2p$ electron to the $\pi_g 2p$ orbital. These states have never been observed experimentally. The contribution of the $^3\Pi$ state to the 6.1 eV transition is considered unimportant because of the triplet→singlet character of the latter and the contribution of the $^1\Pi$ state is likely to be relatively small because of the "buried" nature of the $\sigma_g 2p$ orbital.

A further argument favoring the reassignment of the 6.1 eV transition is the energy dependence of its integral cross section. Our determinations gave 0.21 Å^2 at 15 eV, 0.094 Å^2 at 20 eV and 0.038 Å^2 at 45 eV (see Table I). This rather rapid decrease is characteristic of spin-forbidden transitions.[29]

IV. CONCLUSIONS

The three optically allowed transitions at 8.3 ($X\,^3\Sigma_g^- \rightarrow B\,^3\Sigma_u^-$), 9.97 ("longest" band), and 10.29 eV ("second" band) show angular dependences similar to those observed on optically allowed transitions for other molecules.[30] These observations support the following general rule: The ratio of the differential cross sections of two optically allowed transitions of the same molecule varies by no more than an order of magnitude and usually less as the scattering angle increases from 10 to 90°. The condition for the validity of this rule is that the impact energy be between 10–50 eV above the threshold for the transitions being compared. In addition, we have observed the two transitions: $X\,^3\Sigma_g^- \rightarrow a\,^1\Delta_g$ and $X\,^3\Sigma_g^- \rightarrow b\,^1\Sigma_g^+$. As expected, they show the angular dependencies characteristic of spin forbidden transitions. By this we mean that they are less sharply peaked in the forward direction than optically allowed transitions and furthermore that the ratios of their differential cross sections to that of an optically allowed transition in the same molecule increase by an order of magnitude or more as the scattering angle increases from 10° to 90°. Finally, the identification of the absorption continuum peaking at 6.1 eV as due to the $X\,^3\Sigma_g^- \rightarrow c\,^1\Sigma_u^-$ transition further extends the validity of this rule and is an added illustration of the usefulness of angular distributions not only in detecting but also in identifying the nature of optically forbidden transitions.

* Jet Propulsion Laboratory. Work supported by the National Aeronautics and Space Administration under Contract No. NAS7-100.

† A. A. Noyes Laboratory of Chemical Physics, Division of Chemistry and Chemical Engineering. Contribution No. 4224. Work supported in part by the U.S. Atomic Energy Commission, Report Code No. CALT-767P4-83.

[1] R. H. Garstang, "Forbidden Transitions," in *Atomic and Molecular Processes*, edited by D. R. Bates, (Academic, New York and London 1962), pp. 1–46.

[2] (a) J. F. Noxon, J. Geophys. Res., Space Phys. **75,** 1879 (1970); (b) L. Wallace, Astrophys. J. Suppl. **7,** 165 (1962); (c) G. Herzberg, *Molecular Spectra and Molecular Structure, I. Spectra of Diatomic Molecules*, (Van Nostrand, New York, 1950), p. 178.

[3] W. C. Price and G. Collins, Phys. Rev. **48,** 714 (1935).

[4] T. Tanaka, J. Chem. Phys. **20,** 1728 (1952).

[5] F. R. Gilmore, J. Quant. Spectry. Radiative Transfer **5,** 369 (1965).

[6] J. Geiger and B. Schröder, J. Chem. Phys. **49,** 740 (1968).

[7] (a) E. N. Lassettre, A. Skerbele, M. A. Dillon, and K. J. Ross, J. Chem. Phys. **48,** 5066 (1968); (b) E. N. Lassettre, S. M. Silverman, and M. E. Krasnow, J. Chem. Phys. **40,** 1261 (1964).

[8] A. Skerbele, M. A. Dillon, and E. N. Lassettre, J. Chem. Phys. **49,** 3543 (1968). [See also E. N. Lassettre, Can. J. Chem. **47,** 1733 (1969).]

[9] (a) G. J. Schulz, Phys. Rev. **125,** 229 (1962); (b) G. J. Schulz and J. T. Dowell, Phys. Rev. **128,** 174 (1962).

[10] A. Konishi, K. Wakiya, M. Yamamoto, and H. Suzuki, J. Phys. Soc. Japan **29,** 526 (1970).

[11] (a) A. Kuppermann, J. K. Rice, and S. Trajmar, J. Phys. Chem. **72,** 3894 (1968); (b) S. Trajmar, D. G. Truhlar, and J. K. Rice, J. Chem. Phys. **52,** 4502 (1970).

[12] A. Salop and H. H. Nakano, Phys. Rev. A **2,** 127 (1970).

[13] G. Sunshine, B. B. Aubrey and B. Bederson, Phys. Rev. **154,** 1 (1967).

[14] D. Rapp and P. Englander-Golden, J. Chem. Phys. **43,** 1464 (1965).

[15] S. Trajmar, D. C. Cartwright and W. Williams, Phys. Rev. A, **4,** 1482 (1971).

[16] L. Herzberg and G. Herzberg, Astrophys. J. **105,** 353 (1947).

[17] H. D. Babcock and L. Herzberg, Astrophys. J. **108,** 167 (1948).

[18] (a) R. Ladenburg and C. C. Van Voorhis, Phys. Rev. **43,** 315 (1933); (b) R. Watanabe, E. C. Y. Inn, and M. Zelikoff, J. Chem. Phys. **20,** 1969 (1952); **21,** 1026 (1953); (c) R. W. Ditchburn and D. W. A. Heddle, Proc. Roy. Soc. (London) **A220,** 61 (1953); (d) A. J. Blake, J. H. Carver, and G. N. Haddad, J. Quant. Spectry. and Radiative Transfer **6,** 451 (1966).

[19] (a) G. Herzberg, Can. J. Phys. **30,** 185 (1952); (b) Can. J. Res. **A28,** 144 (1950).

[20] The numbering of v' was later shifted by 1. See H. P. Broida and A. G. Gaydon, Proc. Roy. Soc. **A222,** 181 (1954).

[21] V. Degen and R. W. Nicholls, J. Phys. B **2,** 1240 (1969).

[22] V. Hasson, R. W. Nicholls, and V. Degen, J. Phys. B **3,** 1192 (1970).

[23] W. R. Jarmain and R. W. Nicholls, Proc. Phys. Soc. **90,** 545 (1967).

[24] G. Herzberg, Can. J. Phys. **31,** 657 (1953).

[25] V. Hasson, G. R. Hebert, and R. W. Nicholls, J. Phys. B **3,** 1188 (1970).

[26] K. Watanabe, E. C. Y. Inn, and M. Zelikoff, J. Chem. Phys. **21,** 1026 (1953).

[27] M. Ogawa, J. Chem. Phys. **54,** 2550 (1971).

[28] R. D. Hake, Jr., and A. V. Phelps, Phys. Rev. **158,** 70 (1967).

[29] H. S. W. Massey and E. H. S. Burhop, *Electronic and Ionic Impact Phenomena*, (Oxford U. P., London, 1952), p. 145.

[30] S. Trajmar, J. K. Rice, and A. Kuppermann, Advan. Chem. Phys. **18,** 15 (1970).